Journal of Innovative Technology, Vol. 8, No. 2, pp. 45-58, September 2026
http://doi.org/10.29424/JIT.202609_8(2).0005

Bio-inspired computational intelligence of adaptive differential evolution for harmonics estimation in electrical systems

Naveed Ishtiaq Chaudhary [1], Ali Akram [2], Khizer Mehmood [3*], Zeshan Aslam Khan [4]

ABSTRACT

Various real time nonlinear loads in electrical power system produce harmonic pollution that may cause negative effects on performance of the electrical systems and may results in considerable decreased life of the sensitive equipment. The quality monitoring and reliability assessment of the power systems require parameter estimation of the harmonics. In this study, bio inspired knacks of evolutionary computing through maximum likelihood adaptive differential evolution (MLADE) optimization are exploited to effectively estimate the parameters of power system harmonics represented by multi frequency sinusoidal signal. The performance evaluation of the MLADE in terms of accuracy and robustness is investigated for two case studies considering the harmonic signals normally present in power systems under different noise variations. The reliability assessment of the proposed scheme is carried out through statistical runs based on multiple independent executions. The results of the numerical simulations endorse the accuracy, robustness and reliability of the proposed approach for parameter estimation of power harmonics.

Keywords: Computational intelligence; Evolutionary algorithms; Harmonics; Parameter estimation

1. INTRODUCTION

The considerable use of the solid-state devices and power electronics, such as variable frequency drives (VFDs) and other latest motor start has led to raise the harmonic pollution levels in power system signal during past years. Power quality has become an important issue due to complex power system operation and sensitive load demands. Power quality issues include voltage variations, transients and grounding issues [1]. These harmonics cause different types of negative effects on electrical system such as over voltage, failure of circuit breakers, data loss due to equipment's failure, excessive heat generation in motor winding and rotor, pulsating torque of motor, increase of core (I2R) losses in transformers, malfunctioning of instrumentation, equipment's inefficacy and considerable decreased life of the sensitive equipment [2]. Fig. 1 summarizes common power quality issues.

The occurrence of harmonic pollution in power system considerably decreases the quality of power. Therefore, it is needed to estimate the harmonics parameters to overcome this pollution. Once the harmonic parameters are estimated, such as amplitude, frequency and phase then the harmonic components can be compensated by injecting an appropriate compensating device into a power system [3]these techniques make use of the power of optimization algorithms. Researchers want to improve harmonics estimation's accuracy and effectiveness by utilizing metaheuristic methods, leading to cleaner and more dependable power systems. Offering potential methods for the reduction of harmonic distortions in contemporary electrical systems, this cutting-edge field is still developing. The essential component of feature extraction, which significantly improves the harmonics mitigation efficacy approach, is important to the optimization process. This inquiry includes a thorough analysis of several relevant literature sources as well as an overall evaluation. It employs a variety of methodologies to identify fundamental frequencies and harmonics in the time, space, and frequency domain. Additionally, during the course of this investigation, the integration of signal processing with Meta-Heuristic approaches is examined and evaluated. This investigation provides a thorough overview of modern methods for fundamental frequency and harmonic extraction, together with a thorough analysis and characterization of their benefits and curbs.",",container-title":"Journal of Innovative Technology",",-DOI":"10.29424/JIT.202409_6(2.

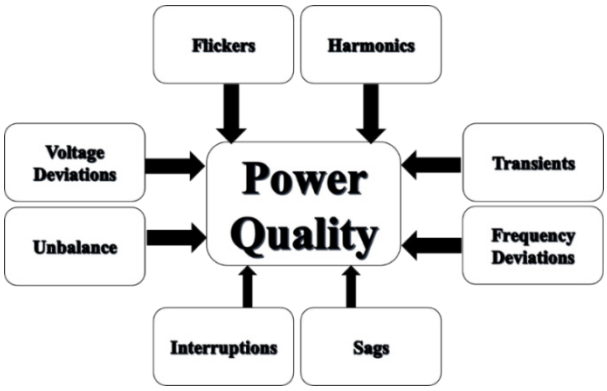


Fig. 1 Problems in Power Quality

Manuscript received April 16, 2026; revised June 29, 2026; accepted July 23, 2026.

[1] Assistant Professor, Graduate School of Intelligent Data Science, National Yunlin University of Science and Technology, Taiwan.
[2] Masters Student, Department of Electrical and Computer Engineering, International Islamic University, Pakistan.
[3*] Assistant Professor (corresponding author), Department of Electrical and Computer Engineering, International Islamic University, Pakistan. (email: khizer.mehmood@iiu.edu.pk)
[4] Associate Professor, International Graduate School of Artificial Intelligence, National Yunlin University of Science and Technology, Taiwan R.O.C.

Different local and global search algorithms were proposed for power systems harmonics estimation. The local-search methods has ease in implementation but suffer from local-minima issue. For example Kalman filtering based estimatiom approach [4], variable leaky least mean square (LMS) algorithm [5], ESPRIT scheme [6], fractional LMS (FLMS) [7], momentum term based FLMS [8] and innovative FLMS that exploits the variable initial value concept in fractional derivative [9]. Whereas, the global-search approaches can deal with the local-minima problem but are computationally expensive. The global-search schemes applied for power system harmonics estimation are marine predator algorithm [10], modified artificial bee colony optimization algorithm [11], harris hawks optimizer [12]harmonics as undesired electrical phenomena, have drawn considerable attention of the research community investigating in design and development of optimal electrical networks. Harmonics affect the power electronics devices with a number of negative impacts, including higher power losses, worse power quality, and interference with other delicate grid connected equipment. An objective function of inter- and sub-harmonics is constructed for joint estimation of amplitude and phase with known frequency. Accurate estimation of the harmonics model is carried out with stupendous knacks of raptor-inspired Harris Hawks optimization algorithm (HHOA, hybrid version of particle swarm optimization and genetic algorithm [13],multi verse optimizer [14], and grey wolf optimizer based heuristic [15].

Recently, maximum likelihood (ML) based DE (MLDE) and ML based adaptive DE (MLADE) were introduced for efficient parameter estimation of multivariable systems [16]. Tariq et al., effectively applied these ML based DE and ADE algorithms for nonlinear system identification [17]. The promising results of ML based bio ispired evolutionary algorithms in terms of accuracy and convergence motivated us to explore their application for harmonics parameter estimation (HPE). In current study, detail investigation in MLDE and MLADE algorithms is conducted for efficient HPE by considering different population length and genertaion size under various disturbance levels. The noticeable contributions are as follows.

- Maximum likelihood differential evolution and adaptive differential evolution algorithms are exploited for parameter estimation of power system harmonics represented through multi frequency sinusoidal signals.
- The detail analyses are conducted through investigating the performance of the proposed scheme by considering different variations in the population length, generation size and noise disturbance.
- The results od simulation studies verify that the evolutionary computational schemes are accurate, convergent and robust for power system harmonics estimation.
- The statistical inferences based on multiple independent executions of the proposed scheme further established the reliability and consistency in case of power systems harmonics estimation.

Remaining article is set as: the HPE model is described in Sec 2. The evolutionary computing paradigm of maximum likelihood based evolutionary algorithms are presented in Sec 3. The simulation results of power systems HPE are provided in Sec 4. Conclusion of the proposed work are listed in Sec 5.

2. HPE Model

A distorted signal can be modeled as sum of higher order harmonics of unknown amplitudes and phases [9]. It is represented in (1)

$$y(i) = \sum_{m=1}^{M} B_m \sin(\omega_m i + \theta_m) + B_{dc} \exp(-\gamma_{dc} i) + \epsilon_i, \quad (1)$$

where M is number of harmonics, ϵ_i is noise, ω_m is the harmonic angular frequency, θ_m is the phase of harmonic signal γ_{dc} is the decaying term and B_m is the distorted voltage signal. Discrete time version of (1) is given in (2)

$$y(i) = \sum_{m=1}^{M} B_m \sin(\omega_m i T_s + \theta_m) + B_{dc} - B_{dc}\gamma_{dc} i T_s + \epsilon_i, \quad (2)$$

T_S is sampling period in (2). Simplify decaying term using Taylor series as given in (3)

$$y(i) = \sum_{m=1}^{M} B_m \sin(\omega_m i T_s + \theta_m) + B_{dc} - B_{dc}\gamma_{dc} i T_s + \epsilon_i, \quad (3)$$

(3) is used to calculate amplitudes and phases of all desired harmonics.

3. Methodology

The MLDE and MLADE based proposed schemes for HPE model are given here. While the graphical abstract of the study is provided in Fig. 2. Fig. 3 shows the block diagram of the HPE model by using the MLDE and MLADE evolutionary algorithms.

3.1 Maximum Likelihood Differential Evolution (MLDE)

The DE is based on a population search mechanism for solution of optimum global problems [18]. Owing to its effectiveness, it is applied on various domains such as remote sensing [19], power dispatch [20], deep learning [21], biomedical image analysis [22], unmanned aerial vehicles [23], visual object tracking [24], and water distribution systems [25]. The recently proposed MLDE algorithm defined the maximum-likelihood based criterion to minimize error. The MLDE achieves global optimum by circulation of three evolutionary operators which are mutation, crossover and selection. For estimation of optimal target vector $\boldsymbol{\delta}_{\text{j.best,h}}$ in HPE model presented in (3).

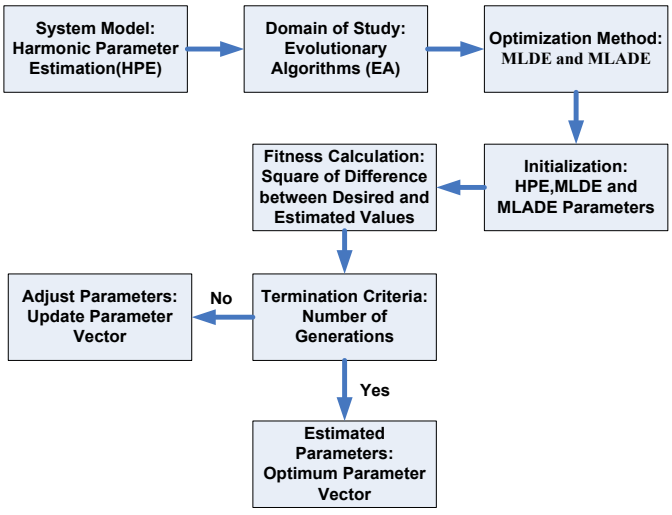


Fig. 2 Graphical abstract of proposed study

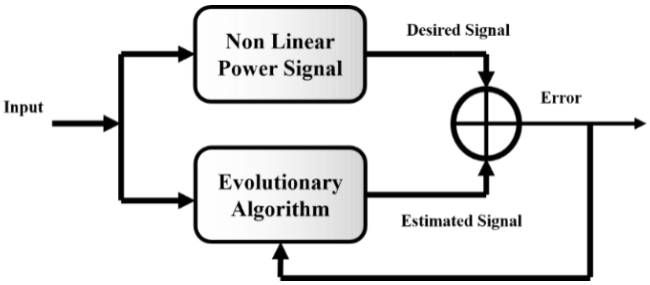


Fig. 3 HPE system model

Let $\aleph_{j,h}$ be the population at generation as given in (4).

$$\aleph_{j,h} = [\boldsymbol{\delta}_{j.1,h}, \boldsymbol{\delta}_{j.2,h}, \dots, \boldsymbol{\delta}_{j.N_p,h}]^T, \quad (4)$$

where N_p is population size. The estimated m^{th} parameter vector at generation is given in (5)

$$\boldsymbol{\delta}_{j.m,h} = [\delta_{j.m,1,h}, \delta_{j.m,2,h}, \dots, \delta_{j.m,D,h}]^T; \quad (5)$$

Each estimated parameter vector in (5) forms a optimation solution for (3).The initial population at h=0 is randomnly chosen as given in (6)

$$\aleph_{j,0} = [\boldsymbol{\delta}_{j.1,0}, \boldsymbol{\delta}_{j.2,0}, \dots, \boldsymbol{\delta}_{j.N_p,0}]^T \quad (6)$$

$$\boldsymbol{\delta}_{j.m,0} = [\delta_{j.m,1,0}, \delta_{j.m,2,0}, \dots, \delta_{j.m,D,0}]^T, \quad (7)$$

$$\delta_{j.m,n,0} = \text{rand}(0,1), m = 1,2, \dots N_p, n = 1,2,..D$$

The mutant vector $\mu_{j.m,h}$ is calculated by taking difference of two target-vectors and adding it to third one as given in (8)

$$\mu_{j.m,h} = \delta_{j.s_1,h-1} + F\cdot(\delta_{j.s_2,h-1} - \delta_{j.s_3,h-1}),\ m = 1,2, \dots N_p, \quad (8)$$

where F is a positive constant. In order to enhance the diversity of population crossover vector $\varepsilon_{j.m,h}$ is generated as given in (9)

$$\varepsilon_{j.m,h} = \begin{cases} \mu_{j.m,n,h} & \text{if } \text{rand}(0,1) \le B \text{ or } m = \text{randperm}(D,1) \\ \delta_{j.m,n,h-1} & \text{otherwise} \end{cases} \quad (9)$$

where B is crossover factor whose value is positive.

The target-vector $\boldsymbol{\delta}_{j.m,h}$ is constucted through selection operator. It calculates crossover vector fitness and target-vector of previous generation $\boldsymbol{\delta}_{j.m,h-1}$ and uses smaller value for construction of target vector. It is presented in (10)

$$\boldsymbol{\delta}_{j.m,h} = \begin{cases} \varepsilon_{j.m,h} & \text{if } J(\varepsilon_{j.m,h}) \le J(\boldsymbol{\delta}_{j.m,h-1}) \\ \delta_{j.m,n,h-1} & \text{otherwise}' \end{cases} \quad (10)$$

Afterwards optimal target vector $\boldsymbol{\delta}_{j.best,h}$ is calculated at generation as given in (11)

$$\boldsymbol{\delta}_{j.best,h} = \boldsymbol{arg\ min}_{\delta_{j.m,h}} \frac{1}{N}\sum_{t=1}^{N}[\boldsymbol{y}_j(t) - \boldsymbol{\tau}_j^T(t)\,\boldsymbol{\delta}_{j.m,h}]^2, m = 1,2, \dots N_p, \quad (11)$$

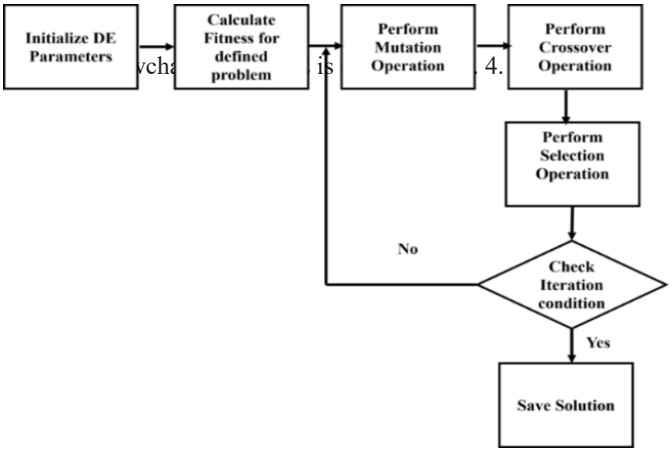


Fig. 4 MLDE Flowchart

3.2 Maximum Likelihood Adaptive DE (MLADE)

Various modifications of the DE were proposed and applied for solution of nonlinear optimization problems [26]. Although there are few similarities in these variants however, the important difference is adaptiveness in mutation and crossover process. Recently, MLADE is proposed in which fitness value is computed by maximum likelihood criterion function [16]. In MLADE, variation is in adaptive factor during mutation and crossover operation according to the generation (H). From (8), mutation factor (F) is fixed and it controls the magnitude of mutation operation. An adaptive mutation factor is incorporated in mutation operation as given in (12) and (13).

$$F_h = F.2^{\beta} \quad (12)$$

$$\beta = \exp\left(1 - \frac{H}{H+1-h}\right) \quad (13)$$

With the increase in generation H, optimal solution is determined and diversity of population is enhanced. To further elevate the accuracy adaptive crossover is incorporated as given is (14).

$$B_h = \begin{cases} \frac{1+\cos(h)}{2}, & h = 1 \text{ or } h = 2r \\ \frac{1+\cos(h-1)}{2}, & h = 2r+1 \end{cases} \quad (14)$$

Replacing these adaptive factors in (8) and (9). The new equations for mutation and crossover are presented in (15) and (16) respectively.

$$\text{Fitness Function} = \text{mean}(\mathbf{y} - \hat{\mathbf{y}})^2 \quad (15)$$

$$\mu_{j.m,h} = \delta_{j.s_1,h-1} + F_h\cdot(\delta_{j.s_2,h-1} - \delta_{j.s_3,h-1}); \quad (16)$$

The selection procedure and optimal target vector calculation are similar to MLDE and given in (17) and (18).

$$\boldsymbol{\delta}_{j.m,h} = \begin{cases} \varepsilon_{j.m,h} & \text{if } J(\varepsilon_{j.m,h}) \le J(\boldsymbol{\delta}_{j.m,h-1}) \\ \delta_{j.m,n,h-1} & \text{otherwise} \end{cases} \quad (17)$$

$$\boldsymbol{\delta}_{\text{j.best,h}} = \boldsymbol{arg\ min}_{\delta_{j.m,h}} \frac{1}{N}\sum_{t=1}^{N}[\boldsymbol{y}_j(t) - \boldsymbol{\tau}_j^T(t)\,\boldsymbol{\delta}_{\text{j.m,h}}]^2, \text{m} = 1,2,\ldots\ \text{N}_\text{p}, \quad (18)$$

The flowchart of MLADE is shown in Fig. 5.

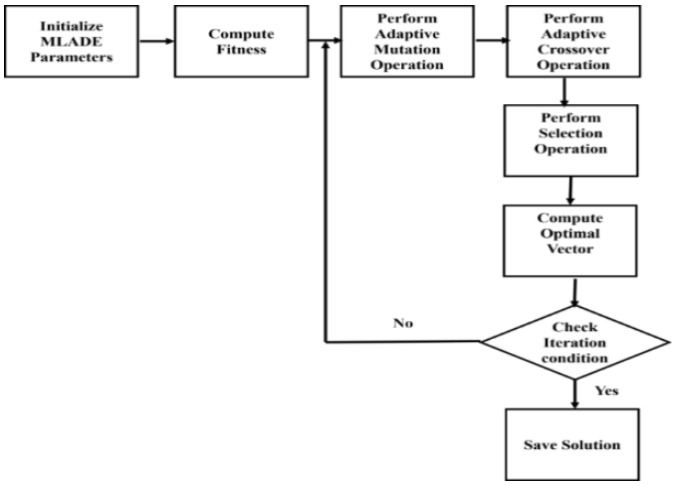


Fig. 5 MLADE Flowchart

Algorithm I: MLADE Pseudocode

Input: Data $\{\boldsymbol{\tau}_\text{j}(1), \boldsymbol{\tau}_\text{j}(2),\ldots,\boldsymbol{\tau}_\text{j}(\text{N})\}$ and $\{\mathbf{y}_\text{j}(1),\mathbf{y}_\text{j}(2),\ldots,\mathbf{y}_\text{j}(\text{N})\}$, Population N_p, mutation factor F_0 and number of generations H. Let generation $\text{h} = 1$.

Output: $\boldsymbol{\delta}_{\text{j,best,h}}$

for $\text{m} = 1{:}\ \text{N}_\text{p}$ **do**
  for $\text{n} = 1{:}\ \text{D}$ **do**
    $\delta_{\text{j.m,n,0}} = \text{rand}(0,1)$;
  End
  $\boldsymbol{\delta}_{\text{j.m,0}} = [\delta_{\text{j.m,1,0}}, \delta_{\text{j.m,2,0}}, \ldots, \delta_{\text{j.m,D,0}}]^{\text{T}}$;
End
$\aleph_{\text{j,0}} = [\boldsymbol{\delta}_{\text{j.1,0}}, \boldsymbol{\delta}_{\text{j.2,0}}, \ldots, \boldsymbol{\delta}_{\text{j.N}_\text{p}\text{,0}}]^{\text{T}}$;
for $\text{h} = 1{:}\,\text{H}$ **do**
  for $\text{m} = 1{:}\ \text{N}_\text{p}$ **do**
    $\text{s}_1 = \text{randperm}\ (\text{N}_\text{p}, 1)$;
    while $\text{s}_1 = \text{m}$ **do**
      $\text{s}_1 = \text{randperm}\ (\text{N}_\text{p}, 1)$;
    End
    $\text{s}_2 = \text{randperm}\ (\text{N}_\text{p}, 1)$;
    while $\text{s}_2 = \text{m}$ or $\text{s}_2 = \text{s}_1$ **do**
      $\text{s}_2 = \text{randperm}\ (\text{N}_\text{p}, 1)$;
    End
    $\text{s}_3 = \text{randperm}\ (\text{N}_\text{p}, 1)$; **while** $\text{s}_3 = \text{m}$ or $\text{s}_3 = \text{s}_1$ or $\text{s}_3 = \text{s}_2$ **do**
    $\text{s}_3 = \text{randperm}\ (\text{N}_\text{p}, 1)$;
  End
end
$\beta = \exp\left(1 - \frac{\text{H}}{\text{H}+1-\text{h}}\right)$; $\text{F}_\text{h} = \text{F}_0 . 2^{\beta}$; $\mu_{\text{j.m,h}} = \delta_{\text{j.s}_1\text{,h}-1} + \text{F}_\text{h} \cdot (\delta_{\text{j.s}_2\text{,h}-1} - \delta_{\text{j.s}_3\text{,h}-1})$;
  if $\text{h} = 1$ or $\text{h} = 2\text{r}$ **then**
    $\text{B}_\text{h} = \frac{1+\cos(\text{h})}{2}$;
  Else
    $\text{B}_\text{h} = \frac{1+\cos(\text{h}-1)}{2}$;
  End

$\boldsymbol{\mu}_{j.m,h} = [\mu_{j.m,1,h}, \mu_{j.m,2,h}, \dots, \mu_{j.m,D,h}]^T$; $\boldsymbol{\delta}_{j.m,h-1} = [\delta_{j.m,1,h-1}, \delta_{j.m,2,h-1}, \dots, \delta_{j.m,D,h-1}]^T$;
for n = 1: D **do**
  if rand(0, 1) ⩽ B_h or n = randperm (D, 1) **then**
    $\varepsilon_{j.m,n,h} = \delta_{j.m,n,h}$;
  Else
    $\varepsilon_{j.m,n,h} = \delta_{j.m,n,h-1}$;
  End
End
  $\boldsymbol{\varepsilon}_{j.m,h} = [\varepsilon_{j.m,1,h}, \varepsilon_{j.m,2,h}, \dots, \varepsilon_{j.m,D,h}]^T$;
  $J(\boldsymbol{\varepsilon}_{j.m,h}) = \frac{1}{N}\sum_{t=1}^{N}[\boldsymbol{y}_j(t) - \boldsymbol{\tau}_j^T(t)\,\boldsymbol{\varepsilon}_{j.m,h}]^2$;
  $J(\boldsymbol{\delta}_{j.m,h-1}) = \frac{1}{N}\sum_{t=1}^{N}[\mathbf{y}_j(t) - \boldsymbol{\tau}_j^T(t)\,\boldsymbol{\delta}_{j.m,h-1}]^2$;
If $J(\boldsymbol{\varepsilon}_{j.m,h}) > J(\boldsymbol{\delta}_{j.m,h-1})$ **then**
  $\boldsymbol{\delta}_{j.m,h} = \boldsymbol{\varepsilon}_{j.m,h}$;
Else
  $\boldsymbol{\delta}_{j.m,h} = \boldsymbol{\delta}_{j.m,h-1}$;
End
$J(\boldsymbol{\delta}_{j.m,h}) = \frac{1}{N}\sum_{t=1}^{N}[\boldsymbol{y}_j(t) - \boldsymbol{\tau}_j^T(t)\,\boldsymbol{\delta}_{j.m,h}]^2$;
$\boldsymbol{\delta}_{j.best,h} = \boldsymbol{arg\ min}_{\boldsymbol{\delta}_{j.m,h}}\ J(\boldsymbol{\delta}_{j.m,h})$;
End

4. SIMULATIONS AND PERFORMANCE ANALYSIS

The proposed algorithms are evaluated in detail through fitness or merit function given in (19).

$$y(i) = \sum_{m=1}^{M} B_m \sin(\omega_m i + \theta_m) + \tag{16}$$

Here **y** and $\hat{\mathbf{y}}$ are the desired and estimated responses. The parameters setting for MLDE, MLADE, harris hawks optimization (HHO) [27], reptile search algorithm (RSA) [28], and whale optimization algorithm (WOA) [29] are given in Table 1.

Table 1 MLDE, HHO, RSA, WOA and MLADE settings

Algorithms	Parameter settings
MLDE	Decision variables=10,Upper Bound=3, Lower Bound=0, Probability of Crossover=0.8, Mutation-Factor=0.25
HHO	Decision variables=10, Upper Bound=3, Lower Bound=0, Rabbit energy [0,2]
RSA	Decision variables=10, Upper Bound=3, Lower Bound=0, alpha = 0.1, beta = 0.1
WOA	Decision variables=10, Upper Bound=3, Lower Bound=0, a = [2 0]
MLADE	Decision variables=10, Upper Bound=3, Lower Bound=0, Probability of Crossover=adaptive, Mutation-Factor=adaptive

The decisions variables defines the amplitudes and phases of electrical harmonic signal. The lower and upper bounds represents the range of values for amplitudes and phases.

4.1. Case 1

The performance of the MLADE is evaluated by considering changed noise levels in HPE model. The per-formance of MLADE through fitness are considered for different generations (H) and populations (Np) which are (30, 60, 90,500) and (20, 40, 60) respectively. The harmonic signal present in industrial loads is taken from [30] and is presented in (20).

$$\begin{aligned} y = {} & 1.05\times\sin(2\times pi\times f_1\times t+70°) \\ & +1.05\times\sin(2\times pi\times f_3\times t+70°) \\ & +0.95\times\sin(2\times pi\times f_5\times t+65°) \\ & +0.97\times\sin(2\times pi\times f_7\times t+85°) \\ & +1.25\times\sin(2\times pi\times f_{11}\times t+93°)+\Delta \end{aligned} \tag{20}$$

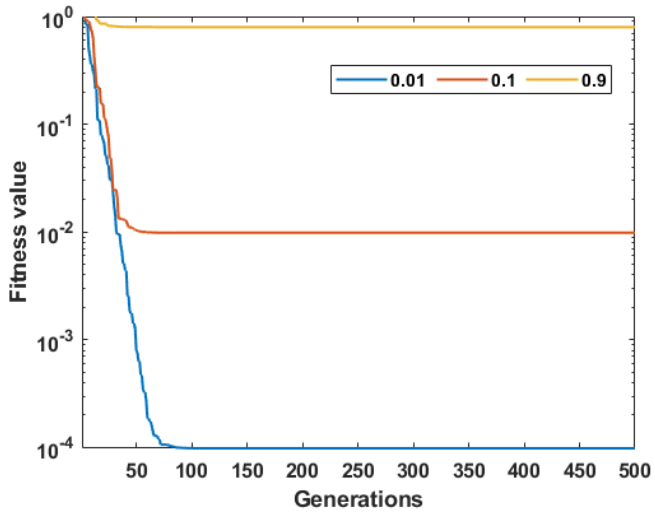
where Δ is the disturbance level.

The detailed results are presented in Table 2 where it is seen that by increasing generations (30, 60, 90,500) and populations (20, 40, 60) fitness value decreases. Moreover, all algorithms have attained minimum fitness value for biggest generation size. It is also perceived that the MLADE has shown superior performance as compared to HHO, RSA, WOA and MLDE for almost all population and generations sizes.

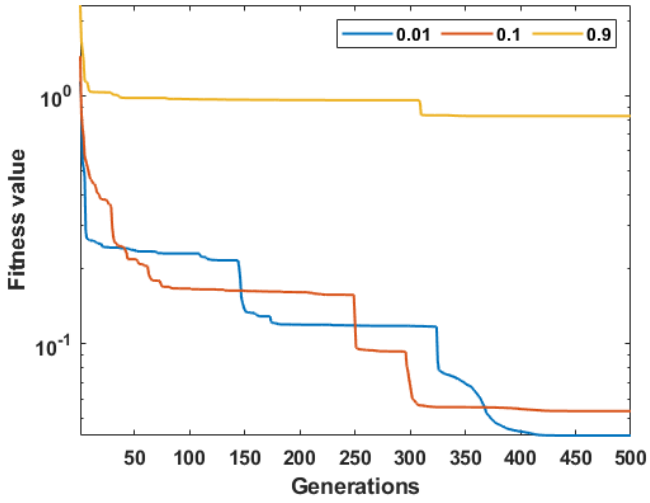
The fitness plots for different generations and population size are given in Fig. 6. Figs 6 (a) – (e) characterize the plots for MLDE,HHO, RSA, WOA and MLADE with H=500, Np=60 and three noise levels (0.01, 0.1, 0.9). It is seen from Figs 6 (a) – (e) that upon increase in noise the fitness values of MLDE, HHO, RSA, WOA and MLADE increases. It is also noted from the Figs 6 (a) – (e) that the MLADE has also achieved lower fitness values for H=500, Np=60 and three noise levels (0.01, 0.1, 0.9).

Table 2 Results of MLDE, HHO, RSA, SCA, WOA and MLADE in case 1

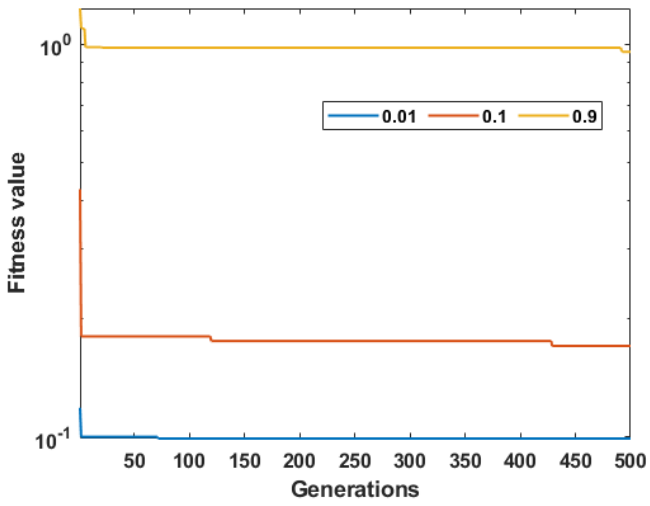
Np	H	Noise	Average Fitness				
			MLDE	HHO	RSA	WOA	MLADE
20	30	0.01	9.33E-02	4.11E-01	1.82E-01	5.86E-01	6.32E-02
		0.1	6.46E-02	4.94E-01	1.87E-01	4.07E-01	8.08E-02
		0.9	8.61E-01	1.31E+00	1.00E+00	1.36E+00	8.65E-01
	60	0.01	4.67E-02	3.10E-01	1.59E-01	3.98E-01	3.75E-03
		0.1	5.51E-02	3.11E-01	1.51E-01	3.66E-01	1.16E-02
		0.9	8.75E-01	1.10E+00	1.05E+00	1.22E+00	8.02E-01
	90	0.01	4.48E-02	2.30E-01	1.64E-01	2.58E-01	3.77E-04
		0.1	4.37E-02	2.73E-01	1.82E-01	3.11E-01	1.07E-02
		0.9	8.29E-01	1.07E+00	1.01E+00	1.14E+00	7.98E-01
	500	0.01	3.60E-02	1.10E-01	1.39E-01	7.29E-02	9.85E-05
		0.1	6.56E-02	1.14E-01	1.71E-01	4.21E-02	9.84E-03
		0.9	8.24E-01	9.06E-01	1.01E+00	8.92E-01	7.97E-01
40	30	0.01	2.07E-02	2.88E-01	1.36E-01	2.80E-01	5.48E-02
		0.1	3.10E-02	3.24E-01	1.53E-01	2.93E-01	6.46E-02
		0.9	8.19E-01	1.11E+00	1.02E+00	1.09E+00	8.37E-01
	60	0.01	1.58E-03	2.25E-01	1.44E-01	2.01E-01	9.99E-04
		0.1	1.12E-02	1.77E-01	1.57E-01	1.58E-01	1.09E-02
		0.9	7.99E-01	1.03E+00	1.02E+00	9.21E-01	7.99E-01
	90	0.01	9.40E-04	1.50E-01	1.57E-01	1.10E-01	1.25E-04
		0.1	1.08E-02	1.63E-01	1.67E-01	8.41E-02	9.86E-03
		0.9	7.98E-01	9.58E-01	9.82E-01	9.03E-01	7.97E-01
	500	0.01	5.13E-04	7.82E-02	1.41E-01	6.77E-03	9.84E-05
		0.1	1.04E-02	8.27E-02	1.56E-01	1.10E-02	9.84E-03
		0.9	7.98E-01	8.69E-01	9.72E-01	8.52E-01	7.97E-01
60	30	0.01	1.58E-02	2.52E-01	1.27E-01	1.91E-01	4.67E-02
		0.1	2.62E-02	1.91E-01	1.39E-01	1.86E-01	5.05E-02
		0.9	8.15E-01	1.01E+00	9.82E-01	1.00E+00	8.37E-01
	60	0.01	2.17E-04	1.37E-01	1.22E-01	9.79E-02	1.09E-03
		0.1	9.97E-03	1.31E-01	1.32E-01	1.22E-01	1.08E-02
		0.9	7.98E-01	9.51E-01	9.63E-01	8.82E-01	7.98E-01
	90	0.01	9.95E-05	1.12E-01	1.27E-01	5.69E-02	1.23E-04
		0.1	9.85E-03	1.30E-01	1.45E-01	1.02E-01	9.86E-03
		0.9	7.97E-01	9.31E-01	9.76E-01	8.70E-01	7.97E-01
	500	0.01	1.72E-04	5.33E-02	1.18E-01	1.87E-02	9.84E-05
		0.1	9.84E-03	6.41E-02	1.64E-01	1.01E-02	9.84E-03
		0.9	7.97E-01	8.50E-01	9.77E-01	8.25E-01	7.97E-01



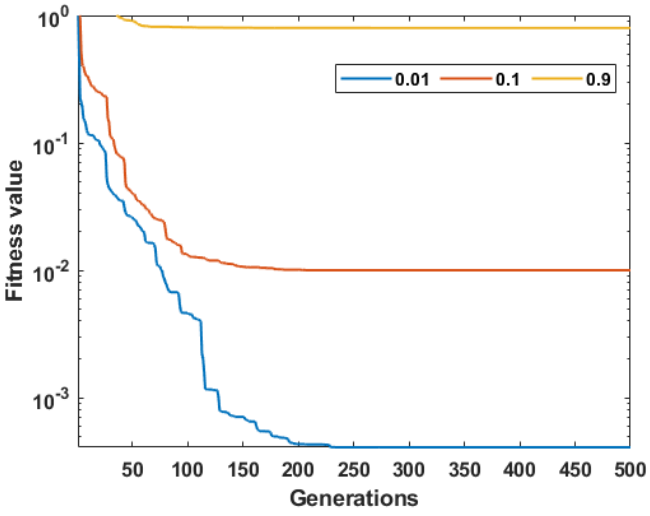
(a) MLDE



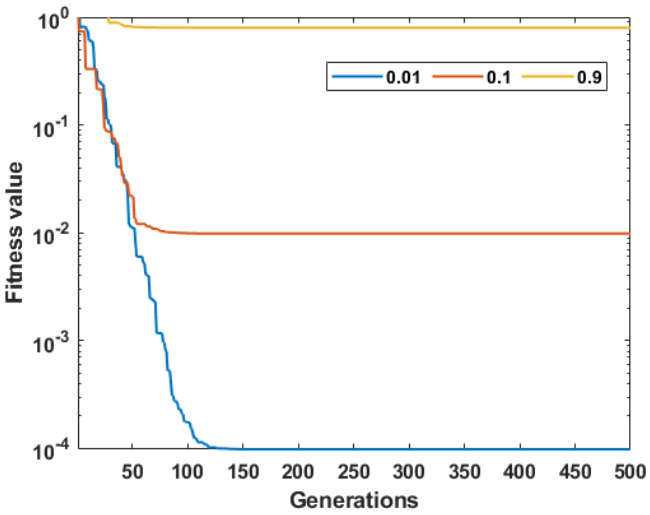
(b) HHO



(c) RSA



(d) WOA



(e) MLADE

Fig. 6 Fitness plots for MLDE,HHO,RSA,WOA and MLADE w.r.t noise

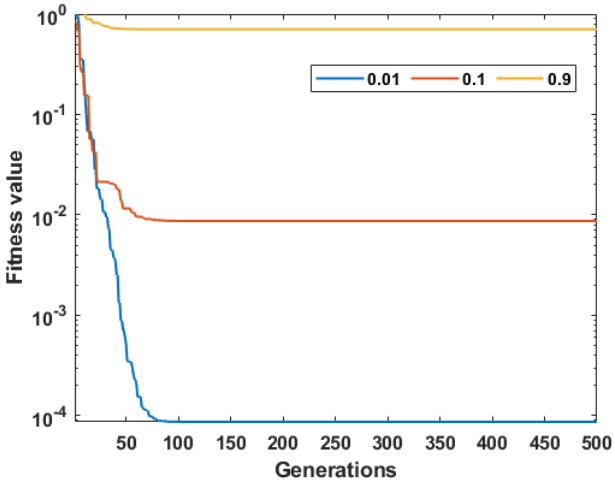
4.2 Case 2

In case 2, MLADE is assessed for populations (20, 40, 60) and generations (30, 60, 90, 500). The actual power system harmonic signal is taken from [31] and is pre-sented in (21).

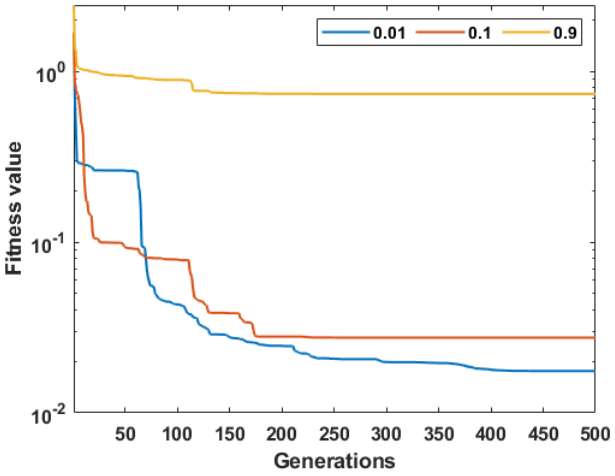
$$y=1.2\times\sin(2\times pi\times f_1\times t+75°) + 0.8\times\sin(2\times pi\times f_3\times t+55°) + 0.2\times\sin(2\times pi\times f_5\times t+45°) + 0.18\times\sin(2\times pi\times f_7\times t+40°) + 0.1\times\sin(2\times pi\times f_{11}\times t+30°)+\Delta \quad (21)$$

The fitness plots for different generations and population size are given in Fig. 7. Figs 7 (a) – (e) characterize the plots for MLDE,HHO, RSA, WOA and MLADE with H=500, Np=60 and

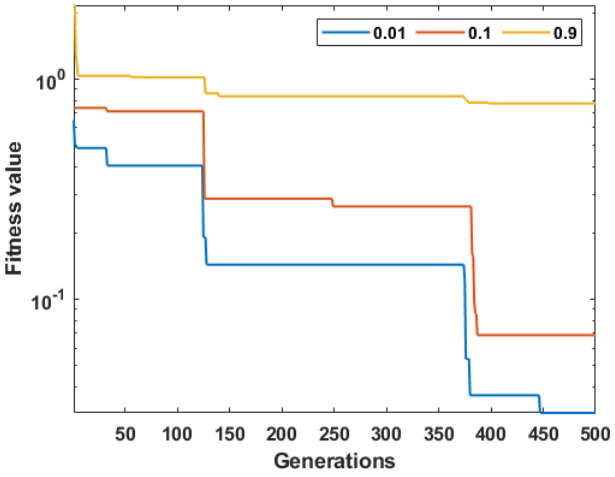
three noise levels (0.01, 0.1, 0.9). It is seen from Figs 7 (a) – (e) that upon increase in noise the fitness values of MLDE, HHO, RSA, WOA and MLADE increases. It is also noted from the Figs 7 (a) – (e) that the MLADE has also achieved lower fitness values for H=500, Np=60 and three noise levels (0.01, 0.1, 0.9).



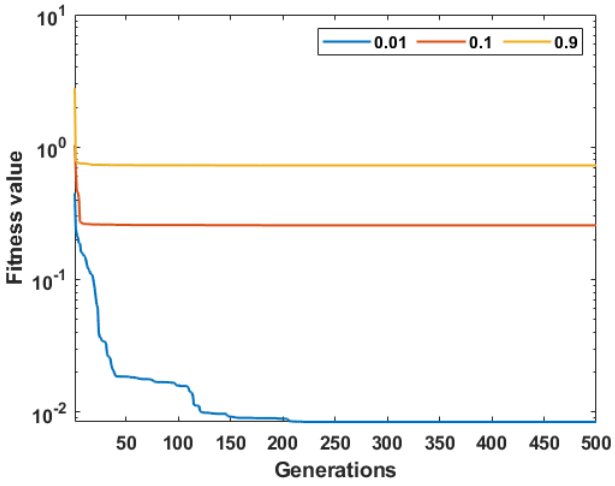
(a) MLDE



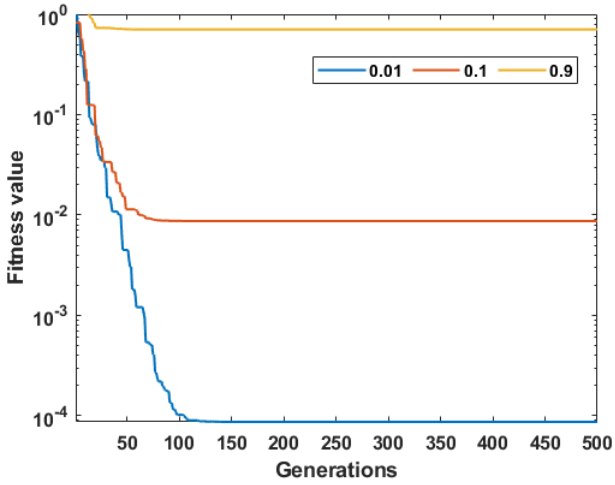
(b) HHO



(c) RSA



(d) WOA



(e) MLADE

Fig. 7 Fitness plots for MLDE, HHO, RSA, WOA and MLADE w.r.t noise

4.3 Sub and Interharmonics investigation

In sub and interharmonics MLADE is evaluated for population (60) and generation (500). The actual power signal is taken from [32] and is presented in (22).

$$\begin{aligned} y = {} & 0.505\times\sin(2\times pi\times f_{sub}\times t+75^\circ) \\ & + 1.5\times\sin(2\times pi\times f_{1}\times t+80^\circ) \\ & + 0.5\times\sin(2\times pi\times f_{3}\times t+60^\circ) \\ & + 0.25\times\sin(2\times pi\times f_{int\,1}\times t+65^\circ) \\ & + 0.35\times\sin(2\times pi\times f_{int\,2}\times t+20^\circ) \\ & + 0.2\times\sin(2\times pi\times f_{5}\times t+45^\circ) \\ & + 0.15\times\sin(2\times pi\times f_{7}\times t+36^\circ) \end{aligned} \tag{22}$$

$$+ 0.1\times\sin(2\times pi\times f_{11}\times t+30^{\circ})$$

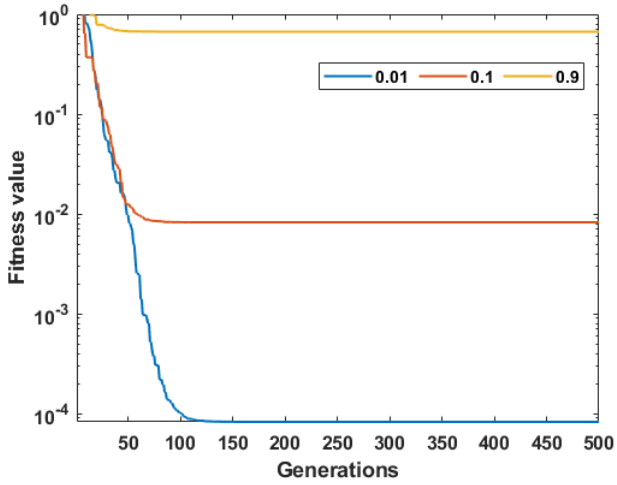
$$+ 0.5\times\exp(-5\times t)+ \Delta$$

The detailed results are offered in Table 3 where it is seen that by increasing noise distubance (0.01, 0.1, 0.9) fitness value increases. Moreover, all algorithms have attained minimum fitness value for lowest noise disturbance level of 0.01. It is also apparent that the MLADE estimates the best weights values as compared to HHO, RSA, WOA and MLDE for almost all noise disturbance levels.

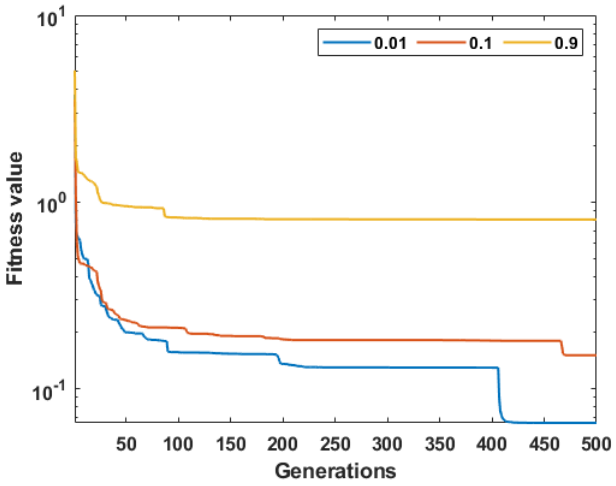
The fitness plots for different generations and population size are given in Fig. 8. Figs 8 (a) – (e) characterize the plots for MLDE,HHO, RSA, WOA and MLADE with H=500, Np=60 and three noise levels (0.01, 0.1, 0.9). It is realized from Figs 8 (a) – (e) that upon increase in noise the fitness values of MLDE, HHO, RSA, WOA and MLADE increases. It is also distinguished from the Figs 8 (a) – (e) that the MLADE has also achieved lower fitness for all noise levels.

Table 3 Estimated weights analysis of MLDE, HHO, RSA, SCA, WOA and MLADE

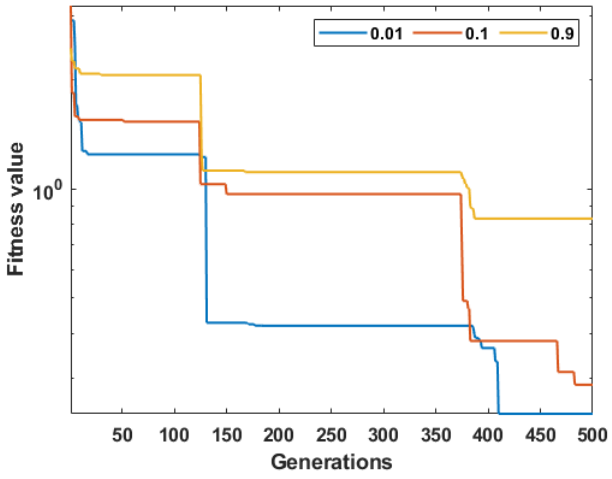
Algorithms	Δ	w_1	w_2	w_3	w_4	w_5	w_6	w_7	w_8	w_9	w_{10}	w_{11}	w_{12}	w_{13}	w_{14}	w_{15}	w_{16}	Average Fitness
MLDE	0.01	0.50	1.50	0.50	0.25	0.35	0.20	0.15	0.10	1.31	1.40	1.04	1.13	0.35	0.77	0.63	0.52	2.2E-04
	0.1	0.48	1.50	0.50	0.26	0.37	0.22	0.14	0.09	1.32	1.39	1.01	1.06	0.40	0.69	0.70	0.47	8.4E-03
	0.9	0.29	1.47	0.52	0.40	0.55	0.39	0.13	0.06	1.40	1.36	0.72	0.65	0.66	0.27	1.42	0.00	6.6E-01
HHO	0.01	0.53	1.38	0.57	0.18	0.41	0.15	0.19	0.13	1.29	1.44	1.09	0.76	0.25	1.06	0.18	1.43	1.1E-01
	0.1	0.55	1.42	0.54	0.26	0.27	0.12	0.28	0.13	1.40	1.40	1.00	1.38	0.39	0.05	0.52	1.25	1.3E-01
	0.9	0.28	1.46	0.39	0.23	0.69	0.35	0.01	0.22	1.69	1.33	0.51	0.68	0.74	0.00	1.35	0.42	7.9E-01
RSA	0.01	0.44	1.20	0.60	0.32	0.51	0.00	0.00	0.17	0.96	1.24	0.92	0.72	0.45	2.06	1.19	1.67	3.8E-01
	0.1	0.37	1.49	0.47	0.11	0.31	0.14	0.03	0.02	1.14	1.16	0.48	1.04	0.17	0.75	0.22	0.39	2.6E-01
	0.9	0.22	1.24	0.67	0.48	0.57	0.21	0.06	0.03	0.71	1.21	0.78	0.79	0.34	0.86	0.96	1.82	9.6E-01
WOA	0.01	0.47	1.51	0.49	0.25	0.35	0.24	0.18	0.11	1.31	1.39	1.01	0.80	0.34	0.63	0.68	0.61	7.7E-02
	0.1	0.45	1.52	0.48	0.28	0.37	0.22	0.14	0.15	1.29	1.39	0.90	0.99	0.43	0.68	0.50	0.12	6.3E-02
	0.9	0.28	1.47	0.51	0.41	0.57	0.39	0.14	0.05	1.43	1.35	0.73	0.48	0.65	0.33	1.39	0.00	7.3E-01
MLADE	0.01	0.50	1.50	0.50	0.25	0.35	0.20	0.15	0.10	1.31	1.40	1.04	1.13	0.35	0.77	0.63	0.52	8.2E-05
	0.1	0.48	1.50	0.50	0.26	0.37	0.22	0.14	0.09	1.32	1.39	1.01	1.06	0.40	0.69	0.70	0.47	8.2E-03
	0.9	0.29	1.47	0.52	0.40	0.55	0.39	0.13	0.06	1.40	1.36	0.72	0.65	0.66	0.27	1.42	0.00	6.6E-01
True Weights	0.50	1.50	0.50	0.25	0.35	0.20	0.15	0.10	1.39	1.04	0.78	0.62	0.52	1.30	1.13	0.34		0



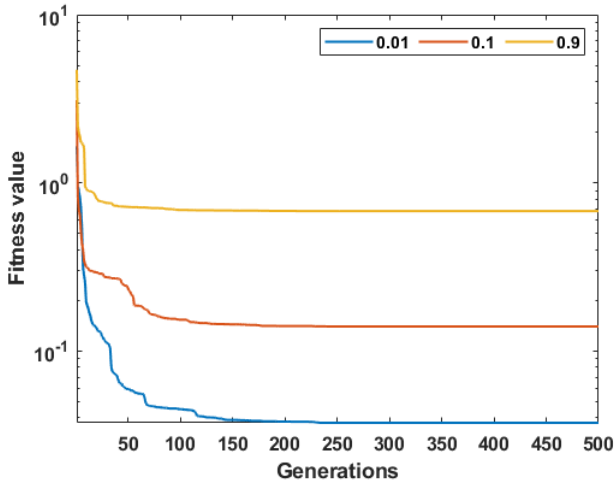
(a) MLDE



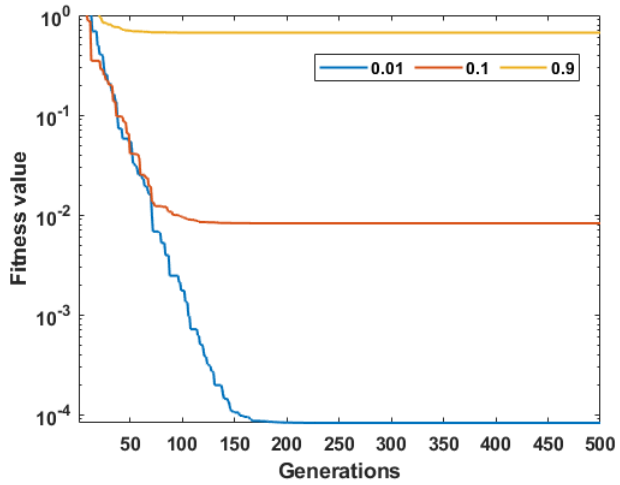
(b) HHO



(c) RSA



(d) WOA

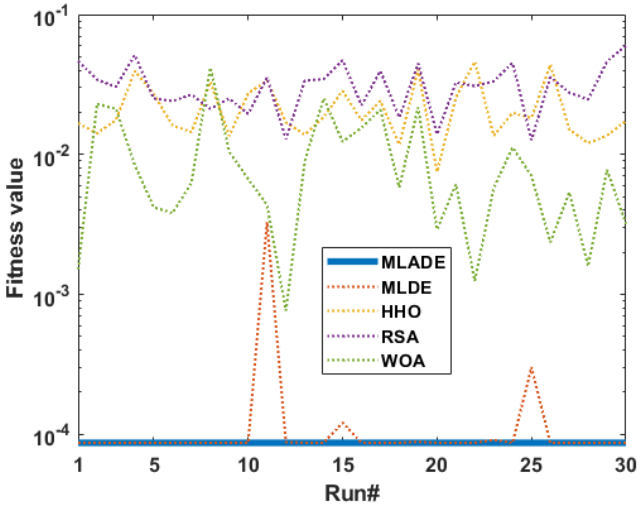


(e) MLADE

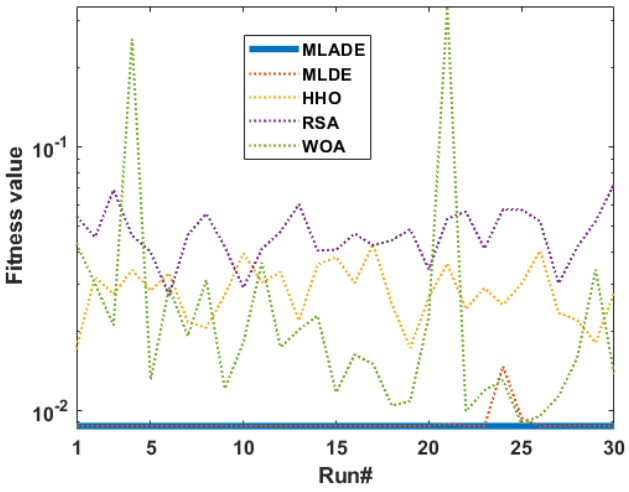
Fig. 8 Fitness plots for MLDE,HHO,RSA,WOA and MLADE w.r.t noise

4.4 Statistical investigation

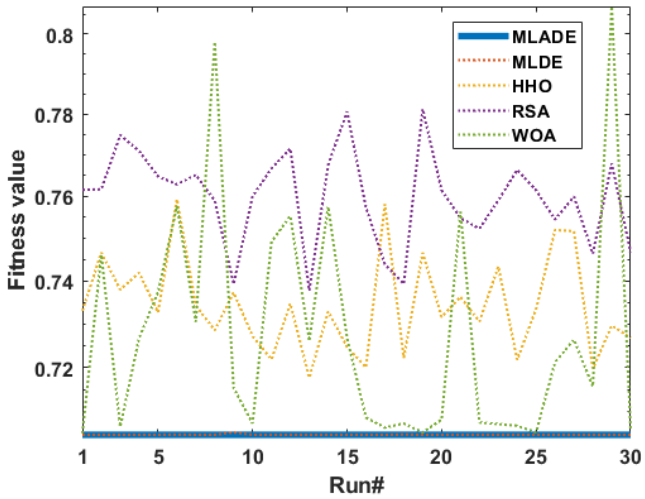
The resullts of MLDE, HHO, RSA, WOA and MLADE for autonomous trials are given in Fig. 9 and it is seen that the MLADE is relatively little more convergent than the MLDE, HHO, RSA and WOA algorithms and the optimal fitness achieved by the MLADE is comparable with the other algorithms. It is further seen that performance of both the MLDE, HHO, RSA, WOA and MLADE algoritms degrades a lttle bit for increased noise variance.However, MLADE achieves lowest fitness values for all noise levels.



(a)Disturbance level = 0.01



(b)Disturbance level = 0.1



(c) Disturbance level = 0.9

Fig. 9 Results of autonomous executions of MLDE, HHO, RSA, WOA and MLADE for Np = 60, H = 500

The effectiveness of MLADE is further validated through the Friedman test for repeated measures [33]. The test is performed using average fitness values of MLADE, MLDE, HHO, RSA, and WOA. The calculated p value is 0.0001. As the significant level the calculated p-value is less than 0.05, which indicates that MLADE is statistically significant.

The performance of MLADE is authenticated through average fitness values. The average fitness value for MLADE, MLDE, HHO, RSA, and WOA is considered for all noise levels. It is seen from bar graph given in Fig. 10 that MLADE outperforms MLDE, HHO, RSA and WOA by achieving lowest fitness in all noise levels.

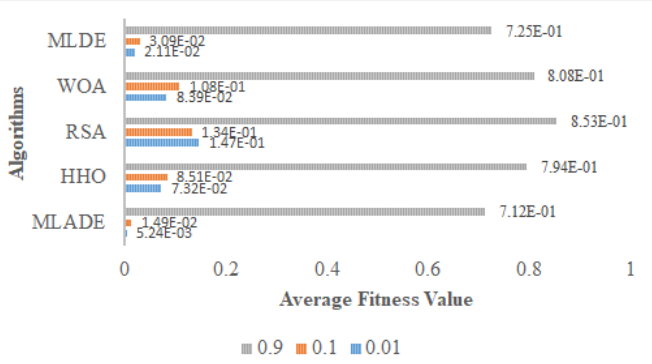


Fig. 10 Results of average fitness of MLDE, HHO, RSA, WOA and MLADE

The boxplots of MLADE, HHO, RSA, WOA and MLDE are given in Fig. 11 displays in terms of average fitness values. It is seen from Fig. 11 that MLADE achieves the lowest median, and lowest first and third quartiles than HHO, RSA, WOA, and MLDE.

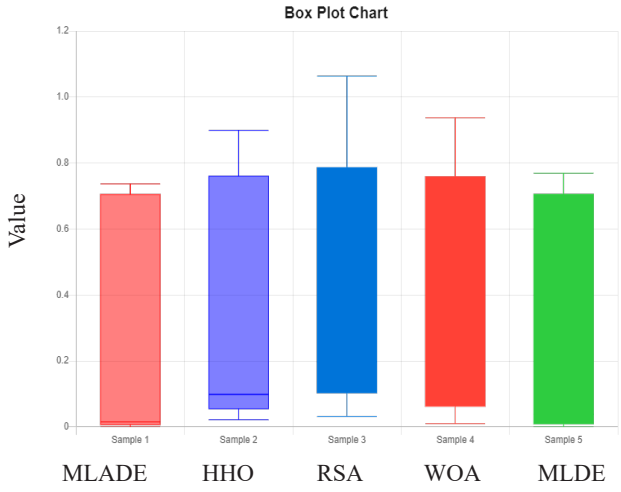


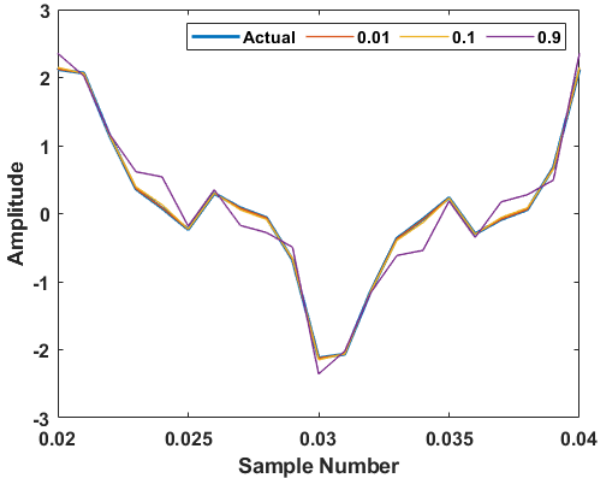
Fig. 11 Results of boxplots for MLADE, HHO, RSA, WOA and MLDE

4.5 Computational Complexity

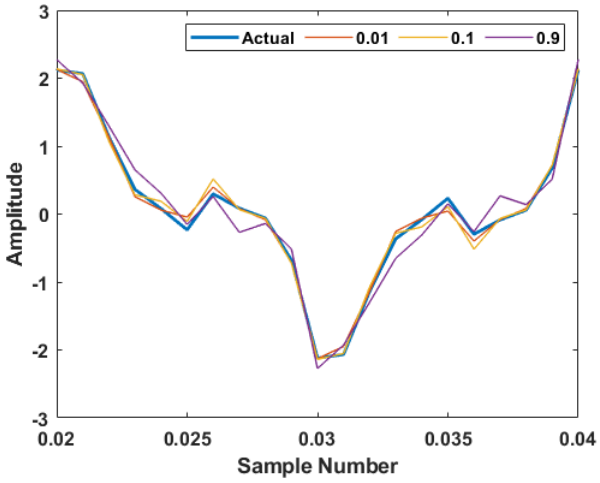
The computational complexity of MLADE is primarily determined by the population (NP) and generation (G) and the number of weights in power signal(F), resulting in an overall complexity of approximately O(NP × G × F).

4.6 Curve fitting through MLDE,HHO,RSA,WOA and MLADE

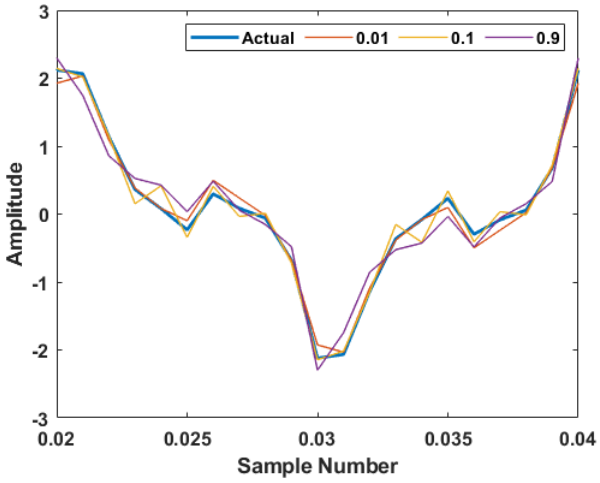
The curve fitting through MLDE, HHO, RSA, WOA and MLADE algorithms with different levels of noise, fixed population and H are given in Fig. 12. It is observed that for all disturbance values MLADE is relatively more close to the actual response than the HHO, RSA, WOA and MLDE algorithms and the optimal amplitudes and phases achieved by MLADE is little better than that of the HHO, RSA, WOA and MLDE for all noise variances.



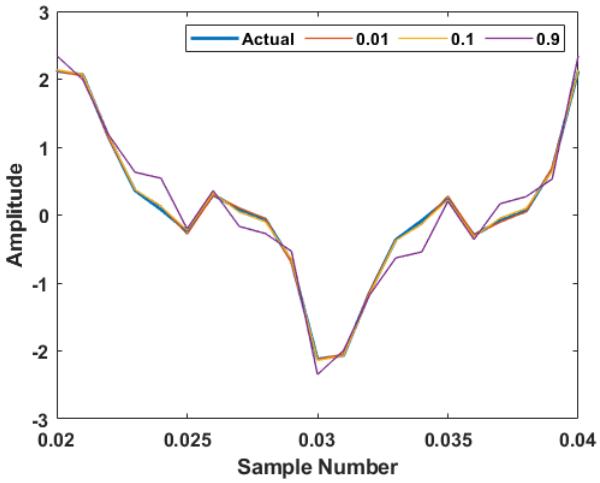
(a)MLDE



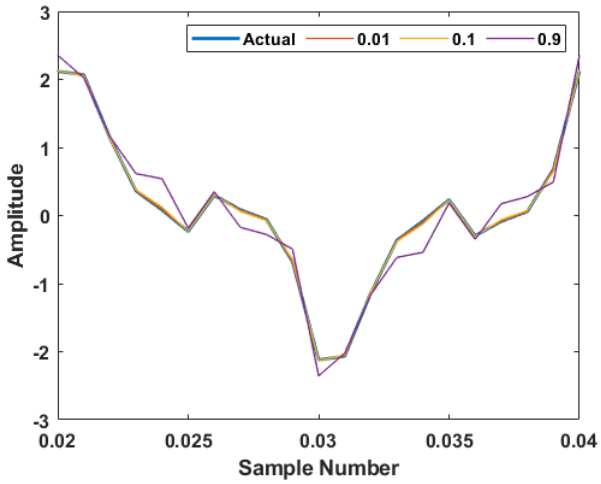
(b)HHO



(c)RSA



(d)WOA



(e)MLADE

Fig. 12 Curve fitting plots of MLDE, HHO, RSA, WOA and MLADE for Np = 60, H = 500

5. CONCLUSIONS

The concluding remarks of the study are:

The maximum likelihood criterion function based DE (MLDE) and ADE (MLADE) algorithms are proposed for harmonics estimation required for quality monitoring and reliability assessment of industrial power systems. The MLDE and MLADE methods effectively estimates the parameters of harmonics under different noise/disturbance conditions. Both algorithms are accurate and convergent but the precision of both evolutionary schemes decreases a little bit by increasing the noise/disturbance level. Moreover, performance improves when population size and generation size increases with a bit more cost. Statistical analysis through multiple autonomous executions validate the reliability and stability of designed scheme for harmonics parameter estimation. The MLADE is relatively little more consistent than the MLDE due to adaptive operation of mutation, crossover and optimal vector generation, but this also decreases the convergence speed of MLADE. Future work will focus on validating the proposed MLADE using experimentally acquired power-quality measurements and publicly available benchmark datasets. Such validation will enable assessment of the algorithm under realistic grid operating conditions and further demonstrate its applicability to online power-quality monitoring and harmonic analysis systems.

Conflicts of Interest: The authors declare no conflict of interest.

Data availability statement: The manuscript has no associated data.

REFERENCES

[1] S. Rönnberg and M. Bollen, “Power quality issues in the electric power system of the future,” *Electr. J.,* vol. **29**, no. 10, pp. 49–61, Dec. 2016, doi: 10.1016/j.tej.2016.11.006.

[2] A. Bakar Waqas, M. Mansoor Ashraf, and Y. Saifullah, “A Hy-

brid Quantum Inspired Particle Swarm Optimization and Least Square Framework for Real-time Harmonic Estimation," *J. Mod. Power Syst. Clean Energy,* vol. **9**, no. 6, pp. 1548–1556, 2021, doi: 10.35833/MPCE.2019.000098.

[3] Naveed Ahmed Malik, Ching-Lung Chang, Naveed Ishtiaq Chaudhary, and Adiqa Kausar Kiani, "A Review on Computational Heuristics in Harmonics Estimation: History, Current top-notch, Challenges and Future Prospects," *J. Innov. Technol.,* vol. **6**, no. 2, Sep. 2024, doi: 10.29424/JIT.202409_6(2).0002.

[4] S. K. Singh, N. Sinha, A. K. Goswami, and N. Sinha, "Several variants of Kalman Filter algorithm for power system harmonic estimation," *Int. J. Electr. Power Energy Syst.,* vol. **78**, pp. 793–800, Jun. 2016, doi: 10.1016/j.ijepes.2015.12.028.

[5] P. K. Ray, P. S. Puhan, and G. Panda, "Real time harmonics estimation of distorted power system signal," *Int. J. Electr. Power Energy Syst.,* vol. **75**, pp. 91–98, Feb. 2016, doi: 10.1016/j.ijepes.2015.08.017.

[6] E. Santos, M. Khosravy, M. A. A. Lima, A. S. Cerqueira, and C. A. Duque, "ESPRIT associated with filter bank for power-line harmonics, sub-harmonics and inter-harmonics parameters estimation," *Int. J. Electr. Power Energy Syst.,* vol. **118**, p. 105731, Jun. 2020, doi: 10.1016/j.ijepes.2019.105731.

[7] N. I. Chaudhary, S. Zubair, and M. A. Z. Raja, "A new computing approach for power signal modeling using fractional adaptive algorithms," *ISA Trans.,* vol. **68**, pp. 189–202, May 2017, doi: 10.1016/j.isatra.2017.03.011.

[8] S. Zubair, N. I. Chaudhary, Z. A. Khan, and W. Wang, "Momentum fractional LMS for power signal parameter estimation," *Signal Process.,* vol. **142**, pp. 441–449, Jan. 2018, doi: 10.1016/j.sigpro.2017.08.009.

[9] N. I. Chaudhary, R. Latif, M. A. Zahoor Raja, and J. A. Tenreiro Machado, "An innovative fractional order LMS algorithm for power signal parameter estimation," *Appl. Math. Model.,* vol. **83**, pp. 703–718, Jul. 2020, doi: 10.1016/j.apm.2020.03.014.

[10] K. M. Cheema et al., "Knacks of marine predator heuristics for distributed energy source-based power systems harmonics estimation," *Heliyon,* vol. **10**, no. 15, p. e35776, Aug. 2024, doi: 10.1016/j.heliyon.2024.e35776.

[11] Y. Kabalci, S. Kockanat, and E. Kabalci, "A modified ABC algorithm approach for power system harmonic estimation problems," *Electr. Power Syst. Res.,* vol. **154**, pp. 160–173, Jan. 2018, doi: 10.1016/j.epsr.2017.08.019.

[12] N. A. Malik, C.-L. Chang, N. I. Chaudhary, M. A. Z. Raja, and C.-M. Shu, "Inter- and sub-harmonics estimation: Treatise on raptor-inspired Harris Hawks collective wisdom," *Int. J. Mod. Phys. C,* vol. **35**, no. 12, p. 2450158, Dec. 2024, doi: 10.1142/S0129183124501584.

[13] Y. Xi et al., "Harmonic estimation in power systems using an optimised adaptive Kalman filter based on PSO-GA," *IET Gener. Transm. Distrib.,* vol. **13**, no. 17, pp. 3968–3979, Sep. 2019, doi: 10.1049/iet-gtd.2018.6148.

[14] A. Haseeb, U. Waleed, M. M. Ashraf, F. Siddiq, M. Rafiq, and M. Shafique, "Hybrid Weighted Least Square Multi-Verse Optimizer (WLS–MVO) Framework for Real-Time Estimation of Harmonics in Non-Linear Loads," *Energies,* vol. **16**, no. 2, p. 609, Jan. 2023, doi: 10.3390/en16020609.

[15] M. Abdullah, T. N. Malik, M. Ashraf, M. A. Shah, Q. Iqbal, and M. Sabir, "Optimal Evaluation of Power System Harmonics in Smart Grid Based on Grey Wolf Optimizer," *in 2020 3rd International Conference on Computing, Mathematics and Engineering Technologies (iCoMET),* Sukkur, Pakistan: IEEE, Jan. 2020, pp. 1–6. doi: 10.1109/iCoMET48670.2020.9074102.

[16] T. Cui, L. Xu, F. Ding, A. Alsaedi, and T. Hayat, "Maximum likelihood-based adaptive differential evolution identification algorithm for multivariable systems in the state-space form," *Int. J. Adapt. Control Signal Process.,* vol. **34**, no. 11, pp. 1658–1676, Nov. 2020, doi: 10.1002/acs.3169.

[17] H. B. Tariq, N. I. Chaudhary, Z. A. Khan, M. A. Z. Raja, K. M. Cheema, and A. H. Milyani, "Maximum-Likelihood-Based Adaptive and Intelligent Computing for Nonlinear System Identification," *Mathematics,* vol. **9**, no. 24, p. 3199, Dec. 2021, doi: 10.3390/math9243199.

[18] K. V. Price, "Differential Evolution," *in Handbook of Optimization, vol. 38, I. Zelinka, V. Snášel, and A. Abraham, Eds.,* in Intelligent Systems Reference Library, vol. **38**. , Berlin, Heidelberg: Springer Berlin Heidelberg, 2013, pp. 187–214. doi: 10.1007/978-3-642-30504-7_8.

[19] D. Singh, M. Kaur, M. Y. Jabarulla, V. Kumar, and H.-N. Lee, "Evolving Fusion-Based Visibility Restoration Model for Hazy Remote Sensing Images Using Dynamic Differential Evolution," *IEEE Trans. Geosci. Remote Sens.,* vol. **60**, pp. 1–14, 2022, doi: 10.1109/TGRS.2022.3155765.

[20] M. Niu, N. Z. Xu, H. N. Dong, Y. Y. Ge, Y. T. Liu, and H. T. Ngin, "Adaptive Range Composite Differential Evolution for Fast Optimal Reactive Power Dispatch," *IEEE Access,* vol. **9**, pp. 20117–20126, 2021, doi: 10.1109/ACCESS.2021.3053640.

[21] Z. Tan and K. Li, "Differential evolution with mixed mutation strategy based on deep reinforcement learning," *Appl. Soft Comput.,* vol. **111**, p. 107678, Nov. 2021, doi: 10.1016/j.asoc.2021.107678.

[22] L. Liu et al., "Performance optimization of differential evolution with slime mould algorithm for multilevel breast cancer image segmentation," *Comput. Biol. Med.,* vol. **138**, p. 104910, Nov. 2021, doi: 10.1016/j.compbiomed.2021.104910.

[23] X. Yu, C. Li, and G. G. Yen, "A knee-guided differential evolution algorithm for unmanned aerial vehicle path planning in disaster management," *Appl. Soft Comput.,* vol. **98**, p. 106857, Jan. 2021, doi: 10.1016/j.asoc.2020.106857.

[24] L. Lin and M. Zhu, "Efficient Tracking of Moving Target Based on an Improved Fast Differential Evolution Algorithm," *IEEE Access,* vol. **6**, pp. 6820–6828, 2018, doi: 10.1109/ACCESS.2018.2793298.

[25] F. Zheng, A. C. Zecchin, and A. R. Simpson, "Self-Adaptive Differential Evolution Algorithm Applied to Water Distribution System Optimization," *J. Comput. Civ. Eng.,* vol. **27**, no. 2, pp. 148–158, Mar. 2013, doi: 10.1061/(ASCE)CP.1943-5487.0000208.

[26] Bilal, M. Pant, H. Zaheer, L. Garcia-Hernandez, and A. Abraham, "Differential Evolution: A review of more than two decades of research," *Eng. Appl. Artif. Intell.,* vol. **90**, p. 103479,

Apr. 2020, doi: 10.1016/j.engappai.2020.103479.

[27] A. A. Heidari, S. Mirjalili, H. Faris, I. Aljarah, M. Mafarja, and H. Chen, "Harris hawks optimization: Algorithm and applications," *Future Gener. Comput. Syst.,* vol. **97**, pp. 849–872, Aug. 2019, doi: 10.1016/j.future.2019.02.028.

[28] L. Abualigah, M. A. Elaziz, P. Sumari, Z. W. Geem, and A. H. Gandomi, "Reptile Search Algorithm (RSA): A nature-inspired meta-heuristic optimizer," *Expert Syst. Appl.,* vol. **191**, p. 116158, Apr. 2022, doi: 10.1016/j.eswa.2021.116158.

[29] S. Mirjalili and A. Lewis, "The Whale Optimization Algorithm," *Adv. Eng. Softw.,* vol. **95**, pp. 51–67, May 2016, doi: 10.1016/j.advengsoft.2016.01.008.

[30] N. A. Malik et al., "Parameter estimation of harmonics arising in electrical instruments of smart grids using cuckoo search heuristics," *Front. Energy Res.,* vol. **10**, p. 1059132, Nov. 2022, doi: 10.3389/fenrg.2022.1059132.

[31] N. A. Malik, C.-L. Chang, N. I. Chaudhary, M. A. Z. Raja, and C.-M. Shu, "Astrophysics-based transit search optimization heuristics for parameter estimation of multi-frequency sinusoidal signals," *Mod. Phys. Lett. B,* p. 2450342, Apr. 2024, doi: 10.1142/S0217984924503421.

[32] K. M. Cheema, K. Mehmood, N. I. Chaudhary, Z. A. Khan, M. A. Z. Raja, and A. Nadeem, "Knacks of Evolutionary Mating Heuristics for Renewable Energy Source–Based Power Systems Signal Harmonics Estimation," *Int. J. Energy Res.,* vol. **2024**, no. 1, p. 8871266, Jan. 2024, doi: 10.1155/2024/8871266.

[33] K. Mehmood, Z. A. Khan, N. I. Chaudhary, K. M. Cheema, B. Siddiqui, and M. A. Z. Raja, "Design of chaotic Young's double slit experiment optimization heuristics for identification of nonlinear muscle model with key term separation," *Chaos Solitons Fractals,* vol. **189**, p. 115636, Dec. 2024, doi: 10.1016/j.chaos.2024.115636.